Available online at www.sciencedirect.com
ScienceDirect
Journal of Solid State Chemistry 181 (2008) 37–44
JOURNAL OF SOLID STATE CHEMISTRY
www.elsevier.com/locate/jssc

Trapping phosphate anions inside the $[Ag_4I]^{3+}$ framework: Structure, bonding, and properties of $Ag_4I(PO_4)$

Olga S. Oleneva[a], Maria A. Kirsanova[a], Tatiana A. Shestimerova[a], Nikolay S. Abramchuk[a], Dmitry I. Davliatshin[a], Mikhail A. Bykov[a], Evgeny V. Dikarev[b], Andrei V. Shevelkov[a,*]

[a]*Department of Chemistry, Lomonosov Moscow State University, Russia*
[b]*Department of Chemistry, University at Albany, USA*

Received 3 July 2007; received in revised form 15 October 2007; accepted 22 October 2007
Available online 4 November 2007

Abstract

Orange-red $Ag_4I(PO_4)$ crystallizes in the monoclinic system, space group $P2_1/m$ (No. 11), with the unit cell dimensions $a = 9.0874(6)$ Å, $b = 6.8809(5)$ Å, $c = 11.1260(7)$ Å, $\beta = 109.450(1)^\circ$, and $Z = 4$. The crystal structure is fully ordered; it comprises the silver–iodine three-dimensional positively charged framework hosting the tetrahedral PO_4^{3-} guest anions. The framework features high coordination numbers for iodine and manifold Ag–Ag bonds ranging from 3.01 to 3.46 Å. The Ag–Ag interaction is bonding, it involves silver 4*d* and 5*s* orbitals lying, together with the orbitals of iodine, just below the Fermi level. Though the orbitals of silver and iodine define the conducting properties of the title compound, the interaction between the framework and the guest anions is also important and is responsive to the number of the silver atoms surrounding the PO_4^{3-} tetrahedra. $Ag_4I(PO_4)$ melts incongruently at 591 K and produces a mixture of the silver phosphate and an amorphous phase upon cooling. Pure $Ag_4I(PO_4)$ is a poor conductor with a room temperature conductivity of 3×10^{-6} S m^{-1}. The discrepancies between the properties observed here and those reported previously in the literature are discussed.

Keywords: Silver; Metal–metal interactions; Crystal structure; Frameworks; Ionic conductivity

1. Introduction

The rapid development of nanotechnology has unexpectedly led to the resurrection of the idea to search for effective Ag^+ conductors. High ionic mobility and almost zero discharge make silver-ion conductors irreplaceable in niche applications, such as in nanostructured memory devices [1]. To this date, many different systems have been investigated, and several compounds showing the conductivity above 1 S m^{-1} at room temperature have been discovered; $RbAg_4I_5$ holds a record at 21 S m^{-1} [2]. The search for new silver-ion conductors continues in various chemical systems, which include complex halides, halophosphates, chalcogen-halides, and others [2,3]. In many cases, the property tuning is restricted because the crystal structures frequently remain unknown. In part, this is also true even in the case of $RbAg_4I_5$, for which the details of the crystal structure have been investigated since its discovery in 1967 [4]. Also, the formation of glasses is typical for many silver-ion conducting systems [5].

This paper deals with $Ag_4I(PO_4)$, a compound which existence was established previously in the course of the work on the Ag_3PO_4–AgI system [6]. In that work, the conductivity of $Ag_4I(PO_4)$ was reported and discussed without any data on its crystal structure. Moreover, the synthetic procedure to $Ag_4I(PO_4)$ reported there brings the question whether the sample for the property measurement was phase-pure. Herein, we report on the synthesis, crystal and electronic structure, and properties of crystalline $Ag_4I(PO_4)$, which has been characterized by means of X-ray diffraction, vibrational and impedance spectroscopy, thermal analysis, and high-temperature optical microscopy. In particular, we describe its unusual crystal

*Corresponding author. Fax: +7 495 939 4788.
E-mail address: shev@inorg.chem.msu.ru (A.V. Shevelkov).

0022-4596/$ - see front matter © 2007 Elsevier Inc. All rights reserved.
doi:10.1016/j.jssc.2007.10.027

structure featuring manifold Ag–Ag bonds, bonding within the Ag–I framework, and the interactions between the framework and embedded phosphate anions. We also discuss the discrepancy between the electrical properties observed in our work and those reported previously in the literature.

2. Experimental

2.1. Synthesis

For the preparation of $Ag_4I(PO_4)$, an equimolar mixture of silver iodide and silver phosphate (all >99.99%; total weight approximately 0.5 g) was heated for 5 days at 875 K in a vacuum-sealed silica tube followed by quenching into iced water. A comparison of the diffraction pattern of the sample (Image Plate Guinier Camera G-670 (Huber), Cu$K\alpha_1$ radiation) with the theoretical pattern calculated on the basis of the data obtained during the structure refinement revealed that the sample was phase-pure (see Supplemental data). Single crystals of the title compound were obtained by annealing a mixture of starting materials (1:1 molar ratio, total weight approximately 0.5 g) in a vacuum-sealed silica tube (60 mm length, 6 mm inner diameter) for 5 days at 875 K and then cooling to ambient temperature at a rate of 30 K h^{-1}. Under such conditions, red crystals of $Ag_4I(PO_4)$ were prepared and mechanically selected from the resulting mixture of the target phase, silver orthophosphate and unidentified non-crystalline admixtures.

2.2. Crystal structure determination

A selected single crystal suitable for the X-ray crystallographic analysis was used for structural determination. The X-ray intensity data were measured at 173(2) K (Bruker KRYOFLEX) on a Bruker SMART APEX CCD-based X-ray diffractometer system equipped with a Mo-target X-ray tube ($\lambda = 0.71073$ Å) operated at 1800 W power. The crystals were mounted on a goniometer head with silicone grease. The detector was placed at a distance of 6.140 cm from the crystal. A total of 1850 frames were collected with a scan width of 0.3° in ω and an exposure time of 20 s $frame^{-1}$. The frames were integrated with the Bruker SAINT Software package using a narrow-frame integration algorithm to a maximum 2θ angle of 56.42° (0.75 Å resolution). The final cell constants are based upon the refinement of the XYZ-centroids of several thousand reflections above 20 $\sigma(I)$. Analysis of the data showed negligible decay during data collection. Data were corrected for absorption effects using the empirical method (SADABS) (minimum/maximum apparent transmission are 0.385). The structure was solved and refined by full-matrix least squares procedures on $|F^2|$ using the Bruker SHELXTL (Version 6.12) software package. The coordinates of silver and iodine atoms were found in direct method E maps. The remaining atoms were located after an alternative series of least-squares cycles and difference Fourier maps. All atoms were refined anisotropically. The final refinement cycle was based on 1642 reflections, 107 parameters, and 0 restraints. The final $R1$ value was 0.0265 ($wR2 = 0.0654$) for 1587 reflections [$I > 2\sigma(I)$] ($R1 = 0.0280$, $wR2 = 0.0663$ for 1642 unique reflections) and a goodness-of-fit of 1.214. The details of the data collection and refinement are summarized in Table 1, the atomic parameters are given in Table 2, and important bond distances and valence angles are collected in Table 3.

2.3. Vibrational spectroscopy

Phase-pure $Ag_4I(PO_4)$ and a mixture of compound with KBr were used for recording Raman and IR spectra, respectively. The samples were powdered and pressed into pellets of 3 mm in diameter. The Raman spectrum was collected with the EQUINOX-55 (Bruker) spectrometer equipped with a FRA 160/S Raman attachment. The IR spectrum was recorded using the TENSOR-27 (Bruker) spectrometer. The data collection ranges were 3500–0 cm^{-1} and 4000–400 cm^{-1} for the Raman and IR experiments, respectively, with the resolution of 4 cm^{-1}. For comparison, the Raman and IR spectra were acquired for Ag_3PO_4 using exactly the same procedure and experimental parameters as for $Ag_4I(PO_4)$. The experimental data are collected in Table 4.

2.4. Thermal analysis

DSC measurements were carried out with a pre-calibrated DSC 204F1 Phoenix (Netzsch) device. About

Table 1
Crystal data for $Ag_4I(PO_4)$[a]

Empirical formula	Ag_4IPO_4
Temperature (K)	173(2)
Space group	$P2_1/m$ (no. 11)
Cell parameters (Å, °)	$a = 9.0874(6)$
	$b = 6.8809(5)$
	$c = 11.1260(7)$
	$\beta = 109.450(1)$
Volume (Å^3)	656.00(8)
Z	4
Density (calculated) (g cm^{-3})	6.615
μ (mm^{-1})	16.652
Crystal size (mm)	$0.15 \times 0.13 \times 0.05$
Radiation, λ (Å)	Mo $K\alpha$, 0.71073
Data collection range (°)	$1.94 < \theta < 28.21$
Reflections collected	5534
Independent reflections	1642 [$R_{(int)} = 0.0257$]
Maximum and minimum transmission	0.4898 and 0.1891
Parameters refined	107
$R1$, $wR2$ [$F_0 > 4\sigma(F_0)$]	0.026, 0.065
$R1$, $wR2$ (all data)	0.028, 0.066
Largest diff. peak and hole (e/Å^3)	1.018 and −2.429
G.o.f. on F^2	1.214

[a]Further details of the crystal-structure investigation may be obtained from the Fachinformationszentrum Karlsruhe, 76344 Eggenstein-Leopoldshafen, Germany, on quoting the depository number CSD-418193.

Table 2
Atomic parameters for the structure of $Ag_4I(PO_4)$

Atom	Wykoff	X/a	Y/b	Z/c	U_{eq} (Å^2)[a]
I(1)	*2e*	0.90651(6)	1/4	0.97768(6)	0.0153(1)
I(2)	*2e*	0.94716(7)	1/4	0.43046(6)	0.0211(1)
Ag(1)	*2e*	0.62218(8)	1/4	0.68815(6)	0.0163(1)
Ag(2)	*2e*	0.68250(8)	1/4	0.21247(7)	0.0184(1)
Ag(3)	*4f*	0.64827(6)	0.02601(7)	0.92785(5)	0.0164(1)
Ag(4)	*4f*	0.70976(6)	0.01090(7)	0.46145(5)	0.0195(1)
Ag(5)	*4f*	0.99640(6)	0.03115(8)	0.22093(5)	0.0221(1)
P(1)	*2e*	0.3653(2)	1/4	0.3234(2)	0.0094(4)
P(2)	*2e*	0.3077(2)	1/4	0.7976(1)	0.0094(4)
O(1)	*2e*	0.3543(7)	1/4	0.6755(5)	0.014(1)
O(2)	*2e*	0.5101(7)	1/4	0.4440(6)	0.015(1)
O(3)	*2e*	0.4124(7)	1/4	0.2017(6)	0.013(1)
O(4)	*2e*	0.1295(7)	1/4	0.7654(6)	0.015(1)
O(5)	*4f*	0.7333(5)	0.9355(6)	0.6764(4)	0.0139(8)
O(6)	*4f*	0.3776(5)	0.0657(6)	0.8756(4)	0.0141(8)

[a] U_{eq} is defined as one third of the trace of the orthogonalized U_{ij} tensor.

Table 3
Interatomic distances (Å) and bond angles (°) in the structure of $Ag_4I(PO_4)$

Framework		PO_4 tetrahedra	
I(1)–Ag(3)	2.7063(7) × 2	P(1)–O(2)	1.535(6)
I(1)–Ag(5)	2.9644(8) × 2	P(1)–O(3)	1.550(6)
I(1)–Ag(5)	3.2714(7) × 2	P(1)–O(5)	1.560(5) × 2
I(1)–Ag(1)	3.3927(9)	P(2)–O(1)	1.552(6)
I(2)–Ag(2)	2.7896(9)	P(2)–O(4)	1.537(6)
I(2)–Ag(4)	2.8241(8) × 2	P(2)–O(6)	1.548(4) × 2
I(2)–Ag(5)	2.9321(8) × 2	Framework–anion interactions	
I(2)–Ag(4)	3.4485(8) × 2	O(1)–Ag(4)	2.300(4) × 2
Ag(1)–Ag(3)	3.0204(8) × 2	O(1)–Ag(1)	2.391(6)
Ag(1)–Ag(4)	3.3224(8) × 2	O(2)–Ag(4)	2.409(4) × 2
Ag(1)–Ag(4)	3.4276(8) × 2	O(2)–Ag(1)	2.564(6)
Ag(2)–Ag(4)	3.1599(8) × 2	O(3)–Ag(3)	2.336(3) × 2
Ag(2)–Ag(5)	3.1992(8) × 2	O(3)–Ag(2)	2.418(6)
Ag(2)–Ag(3)	3.4416(9) × 2	O(4)–Ag(5)	2.278(3) × 2
Ag(2)–Ag(3)	3.4574(8) × 2	O(5)–Ag(5)	2.350(4)
Ag(3)–Ag(1)	3.0204(8)	O(5)–Ag(4)	2.386(4)
Ag(3)–Ag(3)	3.083(1)	O(5)–Ag(1)	2.410(4)
Ag(3)–Ag(2)	3.4416(9)	O(6)–Ag(3)	2.348(4)
Ag(3)–Ag(2)	3.4574(8)	O(6)–Ag(3)	2.362(4)
Ag(4)–Ag(2)	3.1599(8)	O(6)–Ag(2)	2.371(4)
Ag(4)–Ag(4)	3.291(1)		
Ag(4)–Ag(1)	3.3224(8)		
Ag(4)–Ag(1)	3.4276(8)		
Ag(5)–Ag(5)	3.012(1)		
Ag(5)–Ag(2)	3.1992(8)		
Angles around phosphorus atoms			
O(2)–P(1)–O(3)	111.0(3)	O(4)–P(2)–O(6)	109.5(2) × 2
O(2)–P(1)–O(5)	108.9(2) × 2	O(6)–P(2)–O(6)	109.9(3)
O(3)–P(1)–O(5)	109.1(2) × 2	O(4)–P(2)–O(1)	111.7(3)
O(5)–P(1)–O(5)	109.9(3)	O(6)–P(2)–O(1)	108.1(2) × 2

10 mg of the title compound were placed in an aluminum crucible and pressed. Samples were heated up to 870 K in an air or argon flow at a heating and cooling rate varying from 3 to 10 K min^{-1} for different measurements. The Proteus Thermal Analysis (Netzsch) program was used for the data processing. The melting and solidification of the phase-pure sample were observed using an HM-4 high-temperature optical microscope (Union Optical). A sample was pressed into a pellet with dimensions 3 × 3 × 0.5 mm and placed onto a heating plate of the microscope. Observations were performed in an argon atmosphere with the heating and cooling rate of 10 K min^{-1}. A pre-calibrated Pt–Pt/Rh thermocouple was used to control temperature with the accuracy of 1 K.

2.5. Conductivity measurements

The phase-pure sample was pressed into a pellet with a diameter of 12 mm, and gold electrodes were deposited onto the pellet. Impedance spectra were recorded in the argon atmosphere in a ProboStat (NorEsc) sample cell using a Beta-N impedance analyzer. A frequency range of 10 mHz–3 MHz was applied in a temperature range of 293–463 K. Measurements were performed with the accuracy of 5%. The ZView programs were used for the data processing.

2.6. Computational details

Tight-binding extended Hückel calculations [7] were performed employing the PC versions [8] of the programs developed by the Hoffman's group at Cornell University. A mesh of 84 k-points in the irreducible wedge of the Brillouin zone was used. The following orbital parameters were taken for the calculations: I, 5s, $H_{ii} = -18.00$, $\zeta = 2.6790$; I, 5p, $H_{ii} = -12.70$, $\zeta = 2.3220$; Ag, 5s, $H_{ii} = -7.56$, $\zeta = 2.2440$; Ag, 5p, $H_{ii} = -3.88$, $\zeta_1 = 2.2440$; Ag, 4d, $H_{ii} = -11.58$, $\zeta_1 = 6.0700$, $\zeta_2 = 2.6630$, $c_1 = 0.55857$, $c_2 = 0.60527$; P, 3s, $H_{ii} = -19.221$, $\zeta = 1.8160$; I, 3p, $H_{ii} = -9.5390$, $\zeta = 1.4780$; O, 2s, $H_{ii} = -32.30$, $\zeta = 2.27500$; O, 2p, $H_{ii} = -14.80$, $\zeta = 2.27500$. The atomic coordinates and the crystal symmetry were taken from the crystal structure refinement without any modifications.

3. Results and discussion

3.1. Synthesis

The synthesized title compound appeared as an orange-red polycrystalline product, which darkens slowly when exposed to air. The analysis of X-ray powder diffraction profile not only confirmed the absence of crystalline admixtures but also allowed us to exclude the possibility of any amorphous byproducts (see Supplemental data). Annealing of the same starting mixture of silver iodide and silver phosphate at 775 K without further quenching, which is very close to the previously reported synthetic conditions [6], yielded the title compound contaminated with small amounts of $Ag_3(PO_4)$ and unidentified amorphous admixtures. This observation together with the literature data on

Table 4
Vibrational spectroscopy data for $Ag_4I(PO_4)$ and Ag_3PO_4

Ag_4IPO_4				Ag_3PO_4			
Raman spectrum		IR spectrum		Raman spectrum		IR spectrum	
ν (cm^{-1}), A[a]	Correlation	ν (cm^{-1}), A	Correlation	ν (cm^{-1}), A	Correlation	ν (cm^{-1}), A	Correlation
1001, w	F_2	1013, s	F_2			1014, s	F_2
959, w	F_2						
921, vs	A_1						
				910, vs	A_1		
908, vs	A_1						
559, vw	F_2	557, s	F_2			559, m	F_2
413, vw	E			408, w	E		
135, vs	ν (Ag–I)						
116, vs	ν (Ag–I)						

[a]vw—very weak, w—weak, m—medium, s—strong, vs—very strong.

the incongruent melting of $Ag_4I(PO_4)$ motivated us to grow crystals from the equimolar melt of the starting materials (see Section 2).

According to the thermal analysis and high-temperature microscopy data, $Ag_4I(PO_4)$ melts at 591(1) K, which is close to the temperature reported in literature [6]. Upon slow (5 K h^{-1}) cooling the sample starts to solidify at 547(1), however, a complete disappearance of a liquid phase is observed only at 488(2) K. No phase transition was observed in the solid state. The X-ray powder diffraction data show that after two cycles of slow heating and cooling the sample does not contain the title compound; instead it presents a dark-yellow mixture of the silver phosphate and unidentified amorphous phase. We therefore conclude that the sample melts incongruently, and the synthesis of the phase-pure sample is only possible by quenching the melt of the exact composition. Obviously, the title compound does not tend to form glasses; however, slow cooling leads to the decomposition with formation of the amorphous admixture of a different composition.

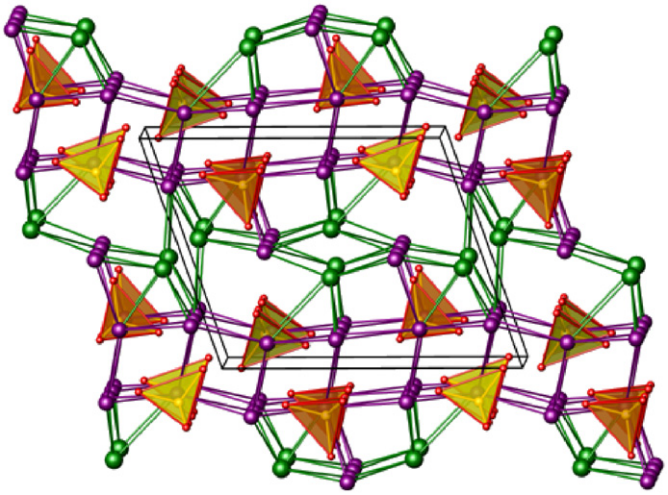

Fig. 1. View of the crystal structure of $Ag_4I(PO_4)$ slightly off the *b*-axis: iodine, green; silver, violet; phosphorus, yellow; oxygen, red; [P(1)O_4] tetrahedron, orange; [P(2)O_4] tetrahedron, yellow.

3.2. Crystal structure

The crystal structure of $Ag_4I(PO_4)$ is built of the complex $[Ag_4I]^{3+}$ three-dimensional polycationic framework encompassing separate tetrahedral PO_4^{3-} guest anions (Fig. 1). Within the silver–iodine network two types of bonds, Ag–I and Ag–Ag, are present. Two crystallographically independent iodine atoms display the same coordination number seven. These atoms have similar coordination polyhedra, which can be considered as distorted monocapped trigonal prisms. The I(1) atom has four short Ag–I distances, 2.71–2.96 Å, and three longer ones, 3.27–3.39 Å. In the case of the I(2) atom five silver atoms lie closer, 2.79–2.93 Å, than other two atoms, 3.45 Å. Thus, the coordination of the I(1) and I(2) atoms is best described as 4 + 3 and 5 + 2 environment, respectively. The coordination of five crystallographically independent silver atoms is quite different. Each silver atom forms from two to eight Ag–Ag bonds at the distances of 3.01–3.46 Å and from one to three Ag–I bonds, such that the coordination number of the silver atoms vary from five to nine (Table 3).

The phosphorus atoms occupy two crystallographically independent positions. The coordination of both phosphorus atoms is very close to regular tetrahedral (P–O = 1.54–1.56 Å; ∠O–P–O = 108.1–111.7°). The linkage between the PO_4^{3-} tetrahedra and the Ag–I framework is achieved through the Ag–O contacts. The Ag–O distances lie in the range of 2.28–2.56 Å, which is comparable with the corresponding distances in silver phosphate, 2.34–2.48 Å [9], while longer than those in silver oxide, 2.05 Å [10]. Each oxygen atom has three Ag–O bonds, except for the O(4) atom that is having two such bonds. This accounts for the difference between the two crystallographically independent tethraheda. Each

tetrahedral PO_4^{3-} anion sits in a quite large cage of silver atoms. However, the $P(1)O_4^{3-}$ tetrahedron connects to 12 silver atoms, while the $P(2)O_4^{3-}$ one is surrounded by 11 metal centers (Fig. 2).

$Ag_4I(PO_4)$ represents a rare example of a compound formed by a fusion of a silver halide and a silver oxo-salt, for which crystal structure is determined. There are only few other examples in the literature [11,12]. Among those, the crystal structure of $Ag_5I(P_2O_7)$ provides the most similarity with the crystal structure of $Ag_4I(PO_4)$. In $Ag_5I(P_2O_7)$ silver and iodine atoms form a framework that trap $P_2O_7^{4-}$ anions [13]. Within the framework the iodine atoms possess a coordination number eight, and the silver atoms form Ag–Ag bonds with the separations ranging from 2.92 to 3.52 Å. However, there is a certain disorder in the latter framework resulting from a partial occupancy of four of seven silver atomic positions. Such a disorder is believed to be responsible for high ionic mobility in $Ag_5I(P_2O_7)$ [6,11]. The positional disorder is even stronger in the $Ag_{16}I_{12}(P_2O_7)$, $Ag_8I_4(V_2O_7)$, and $Ag_{26}I_{18}(W_4O_{16})$ compounds, which crystal structures lack straightforward description because of a complex distribution of partially occupied atoms both within the silver–iodine frameworks and guest anions [12]. $Ag_3Cl(CrO_4)$ provides the only example of a completely ordered crystal structure in this family [13]. In the latter chromate anions occupy voids of a silver–chlorine framework, in which silver has a linear coordination, similar to the coordination of mercury in various host–guest compounds based on the mercury–pnicogen frameworks [14].

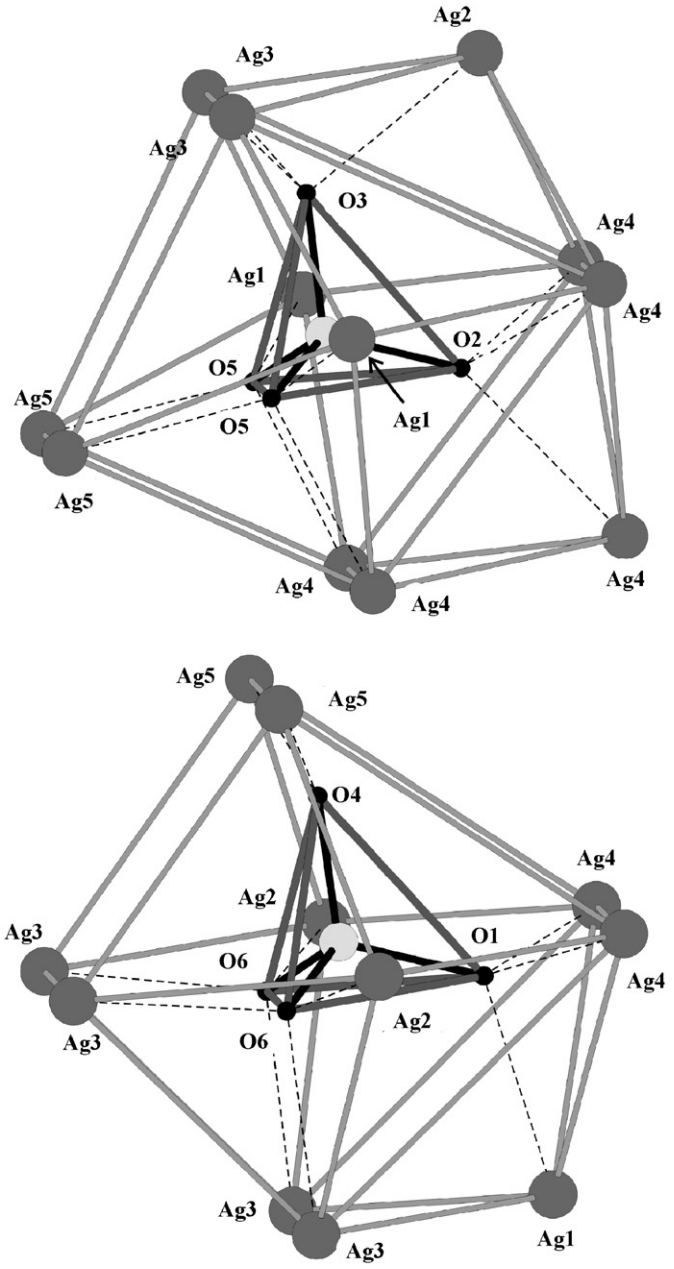

Fig. 2. Surroundings of the $[P(1)O_4]$ (top) and $[P(2)O_4]$ (bottom) tetrahedra by silver atoms of the framework: silver, gray; phosphorus, light gray; oxygen, black. Atomic labeling is in accordance with Table 2.

3.3. Bonding

The bonding in $Ag_4I(PO_4)$ was analyzed qualitatively using the extended Hückel approach [7]. The analysis revealed the significant band gap as well as the fact that the states in vicinity of the Fermi level are mainly constructed from the *d* orbitals of silver and *s* and *p* orbitals of iodine (Fig. 3). The silver *d* orbitals are not fully localized but rather mixed with the valence orbitals of iodine between –14 and –10.5 eV, however, the Ag–I interaction just below the Fermi level is antibonding. A slight Ag–O antibonding interaction is also observed at the same energy, though mainly the valence orbitals of oxygen mix with the valence orbitals of phosphorus (not shown) at lower energy, where two distinct regions of the P–O *s* and *p* interactions are seen at about –17.5 eV and –15.5 eV, respectively. Also, the antibonding interaction of the silver *d* orbirals with the *s*, *p* orbitals of oxygen is present just below the Fermi level, whereas the mixing of the silver *s* and *p* orbitals with the valence orbitals of oxygen is positive and occurs at much lower energy.

Further analysis shows a rather complicated pattern of the Ag–Ag interactions, with the positive and negative regions. It is clear from Fig. 3 that the bonding interaction prevails near the Fermi level. The strength of such an interaction cannot be properly estimated within the frames of the extended Hückel calculations, because the results are quite sensitive to the parameterization chosen. However, the existence of the Ag–Ag bonding is evident from the calculations. Typically, this bonding is attributed to the combination of hybridization and dispersion [15].

The analysis of the atomic charges indicates that all silver atoms bear a positive charge, which varies slightly from one atom to another, still no correlation is observed between the number of the Ag–O, Ag–I, or Ag–Ag bonds and the atomic charges. Taking the analysis of the orbital interactions and the atomic charges together it is plausible to propose the qualitative bonding picture, which includes

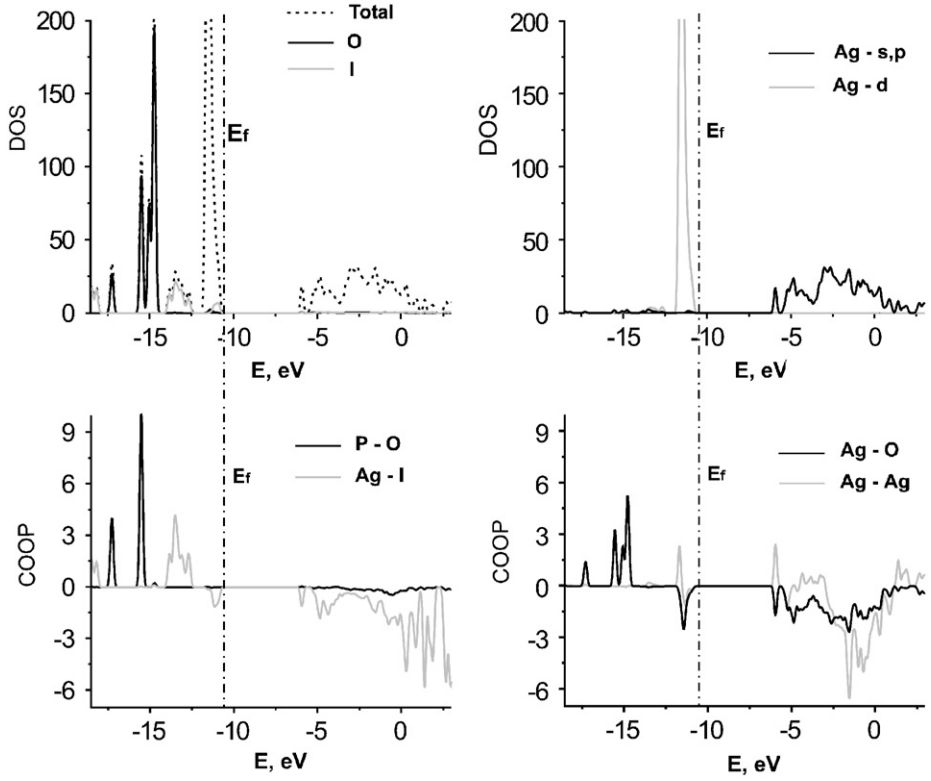

Fig. 3. Density of states (DOS) and crystal orbital overlap population (COOP) for the bandstructure of $Ag_4I(PO_4)$.

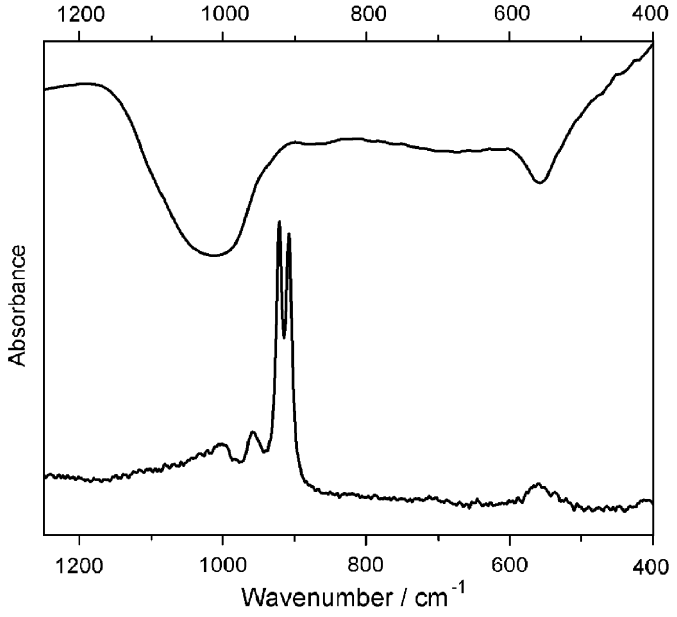

Fig. 4. Portion of IR (top) and Raman (bottom) spectra of $Ag_4I(PO_4)$ between 1250 and 400 cm^{-1}.

the mainly ionic interaction between the covalently bonded Ag–I framework and the PO_4^{3-} tetrahedra.

The vibrational spectroscopy data provide further information on the specific interaction between the Ag–I framework and the PO_4^{3-} anions. The portion of the Raman and IR spectra of $Ag_4I(PO_4)$ is shown in Fig. 4. Vibration frequencies of $Ag_4I(PO_4)$ were compared with the corresponding frequencies of the tetrahedral PO_4^{3-} anion in Ag_3PO_4 (Table 4). The asymmetric vibration frequencies F_2 of $Ag_4I(PO_4)$ coincide with those of Ag_3PO_4, which confirms that PO_4^{3-} anions in the $Ag_4I(PO_4)$ possess almost regular tetrahedral symmetry enabling the triply degenerate vibration. On the contrary, the apparent splitting of the fully symmetric A_1 vibration frequency in the Raman spectrum indicates the existence of two different types of the PO_4^{3-} anions. The observed splitting cannot be a result of the distortion of the $[PO_4]$ tetrahedron, since the A_1 vibration is non-degenerate. Therefore, we attribute the apparent splitting to the difference in the local environment of two types of the $[PO_4]$ tetrahedra. The two tetrahedra differ by the number of the neighboring silver atoms (Fig. 2), 12 for $[P(1)O_4]$ and 11 in the case of $[P(2)O_4]$. We thus conclude that the difference in the number of the positively charged silver atoms provides a sufficient difference in the electrostatic potential around the tetrahedra for the splitting to be observed.

3.4. Conductivity

Our preliminary investigation shows that $Ag_4I(PO_4)$ displays a very moderate, presumably ionic conductivity with a room temperature value of $3\times10^{-6}\,S\,m^{-1}$, which is comparable to the conductivity of AgBr [16] and AgN_3 [17]. The conductivity increases with raising the

temperature, reaching $7 \times 10^{-3}\,S\,m^{-1}$ at 463 K, and the activation energy obtained from the linearization of the $\ln(\sigma T) = f(T^{-1})$ function is 0.47 eV.The observed values contradict with the data for this compound presented in the literature, where the room temperature conductivity is four orders of magnitude higher [6]. We attribute such a discrepancy to the synthetic method used in the literature, where the experimental conditions very likely lead to the formation of the mixture of $Ag_4I(PO_4)$ with an amorphous phase having better ionic conductivity. The analysis of the crystal structure does not point out explicitly the possible mechanism of the ionic conduction. Though the concentration of silver ions is very high, there is no sign of positional disorder and/or phase transition, which are typical indicators of the prospective ionic conductors [18].

3.5. Conclusions

A long-known compound $Ag_4I(PO_4)$ possesses a new type of crystal structure, which relates to the structures of several silver-conducting compounds having the Ag–I framework. This framework features high coordination numbers for the iodine atoms and manifold Ag–Ag bonds. The title compound is unique in the family since its crystal structure is fully ordered, which makes it an excellent object for investigating the structure–properties relationship. $Ag_4I(PO_4)$ devoid of phase transitions, which, together with the lack of disorder, determine its quite low conductivity, only $3 \times 10^{-6}\,S\,m^{-1}$ at room temperature. The investigation of the electronic structure suggests that $Ag_4I(PO_4)$ is a wide-gap semiconductor, therefore, the observed activation energy of 0.47 eV indicates that the conductivity is ionic. Such a low conductivity was measured on well-tested samples, free of contaminations by amorphous phases, which explains a severe discrepancy between the results obtained in this work and those reported in the literature. The investigation of other compounds with different types of the frameworks containing silver–silver bonds, that might lead to the discovery of new silver-ion conductors and help in establishing their structure–property relationship, is currently underway.

Acknowledgment

The authors wish to thank Dr. A.V. Knotko and Dr. S.N. Savin for the conductivity measurements and Dr. V.I. Shtanov for discussion. E.V.D. is grateful to the National Science Foundation for funding the diffractometer (CHE-0619422) at the University at Albany. This work is supported in part by the Russian Foundation of Basic Research.

Appendix A. Supporting information

Supplemental data

A powder XRD pattern for the phase-pure title compound, an ellipsoid presentation of its crystal structure, DTA curves, and reference vibrational spectra for Ag_3PO_4 are available upon request to the corresponding author.

Appendix B. Supplementary materials

Supplementary data associated with this article can be found in the online version at doi:10.1016/j.jssc.2007.10.027.

References

[1] (a) M.N. Kozicki, M. Mitkova, M. Park, M. Balakrishnan, C. Gopalan, Superlattices Microstruct. 34 (2003) 459–465;
(b) M. Mitkova, M.N. Kozicki, J. Non-Cryst. Solids 299–302 (2002) 1023–1027.
[2] S. Lange, T. Nilges, Chem. Mater. 18 (2006) 2538–2544.
[3] (a) S. Lange, M. Bawohl, D. Wilmer, H.W. Meyer, H.D. Wiemhöfer, T. Nilges, Chem. Mater. 19 (2007) 1401–1410;
(b) C.P.M. Oberndofer, M. Jansen, Z. Anorg. Allg. Chem. 633 (2007) 172–175;
(c) H. Naïli, H. Ettis, T. Mhiri, J. Alloys Compd. 424 (2006) 400–407;
(d) M. Onoda, H. Wada, A. Sato, M. Ishii, J. Alloys Compd. 383 (2004) 113–117;
(e) G.D. Tsyrenova, S.F. Solodovnikov, E.G. Khaikina, E.T. Khobrakova, Z.h.G. Bazarova, Z.A. Solodovnikova, J. Solid State Chem. 177 (2004) 2158–2167;
(f) H. Wada, A. Sato, M. Onoda, S. Adams, M. Tansho, M. Ishii, Solid State Ionics 154–155 (2002) 723–727.
[4] (a) S. Geller, Science 157 (1967) 310–312;
(b) S. Hull, D.A. Keen, D.S. Sivia, P. Berastegui, J. Solid State Chem. 165 (2002) 363–371;
(c) K. Funke, R.D. Banhatti, D. Wilmer, R. Dinnebier, A. Fitch, M. Jansen, J. Phys. Chem. A 110 (2006) 3010–3016.
[5] (a) M.A. Ureña, A.A. Piarristeguy, M. Fontana, B. Alonso, Solid State Ionics 176 (2005) 505–512;
(b) N. Dridi, A. Boukhari, J.M. Réau, Mater. Lett. 50 (2001) 302–307;
(c) M. Cutroni, A. Magistris, M. Villa, Solid State Ionics 53–56 (1992) 1232–1236;
(d) J. Liu, J. Portier, B. Tanguy, J. Videau, J. Mater. Lett. 10 (1990) 42–44.
[6] T. Takahashi, S. Ikeda, O. Yamamoto, J. Electrochem. Soc. 18 (1972) 477–482.
[7] J.H. Ammeter, H.B. Bürgi, J.C. Thibeaut, R. Hoffman, J. Am. Chem. Soc. 100 (1978) 3686–3692.
[8] M. Brändle, R. Rytz, G. Calzaferri, BICON-CEDiT, Manual, University of Bern, 1997.
[9] (a) J.M. Newsam, A.K. Cheetham, B.C. Tofield, Solid State Ionics 1 (1980) 377–393;
(b) R. Masse, I. Tordjman, A. Durif, Z. Kristallogr. 144 (1976) 76–81.
[10] P. Niggli, Z. Kristallogr. 57 (1922) 253–299.
[11] S. Adams, A. Preusser, Acta Crystallogr. C 55 (1999) 1741–1743.
[12] (a) J.D. Garrett, J.E. Greedan, R. Faggiani, S. Carbotte, I.D. Brown, J. Solid State Chem. 42 (1982) 183–190;
(b) S. Adams, Z. Kristallogr. 211 (1996) 770–776;
(c) L.Y.Y. Chan, S. Geller, J. Solid State Chem. 21 (1977) 331–347.
[13] J. Curda, E.-M. Peters, W. Klein, M. Jansen, Z. Kristallogr. 216 (2001) 180.
[14] (a) A.V. Olenev, O.S. Oleneva, M. Lindsjö, L.A. Kloo, A.V. Shevelkov, Chem. Eur. J. 9 (2003) 3201–3208;
(b) O.S. Oleneva, T.A. Shestimerova, E.V. Dikarev, A.V. Shevelkov, Angew. Chem. Int. Ed. 45 (2006) 7719–7722;

(c) J.-P. Zou, D.-S. Wu, S.-P. Huang, J. Zhu, G.-C. Guo, J.-S. Huang, J. Solid State Chem. 180 (2007) 805–811.
[15] (a) P. Pyykko, Chem. Rev. 97 (1997) 597–636;
(b) P.K. Mehrotra, R. Hoffmann, Inorg. Chem. 17 (1978) 2187–2189.
[16] J. Maier, Mater. Res. Bull. 20 (1985) 383–392.
[17] C.L. Schmidt, R. Dinnebier, U. Wedig, M. Jansen, Inorg. Chem. 46 (2007) 907–916.
[18] D.A. Keen, J. Phys. Condens. Matter 14 (2002) R819–R857.